Atomic Vibrations and Melting in Plutonium

Andrew C. Lawson, Barbara Martinez, Joyce A. Roberts, James W. Richardson, Jr., and Bard I. Bennett

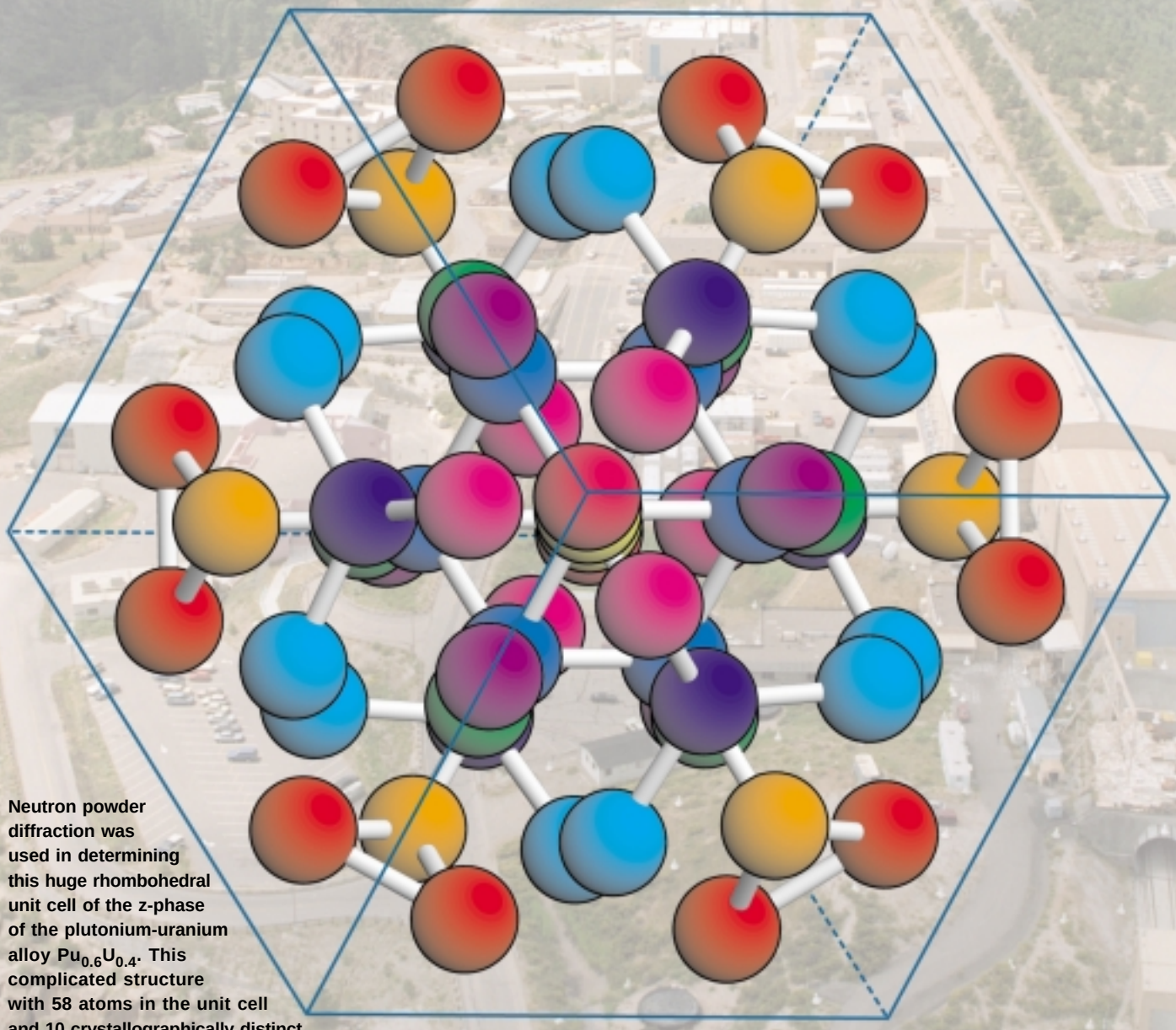

Neutron powder diffraction was used in determining this huge rhombohedral unit cell of the z-phase of the plutonium-uranium alloy $Pu_{0.6}U_{0.4}$. This complicated structure with 58 atoms in the unit cell and 10 crystallographically distinct atom types illustrates the general tendency for complex structures in plutonium and its alloys. The Los Alamos Neutron Scattering Center is shown in the background.
(Crystal structure was reproduced with permission from *Acta Crystallographica* B52, 1996.)

At any temperature, the atoms in a crystalline solid are constantly vibrating about their equilibrium positions. Those positions define the crystal lattice and are ultimately determined by the electronic structure of the solid. As the material heats up, the atoms vibrate about their lattice sites with increasing amplitude until they shake loose and the material melts. The square of the vibrational amplitude is inversely proportional to the strength of the atomic forces that bind each atom to its lattice site. In some materials, including plutonium, the vibrational motion that accompanies heating can cause the electrons to rearrange around the atoms, changing the strength of the interatomic forces. Measuring the atomic vibrations therefore gives information about the strength of these interatomic forces and, ultimately, about the electronic structure and its variation with temperature and applied pressure.

The response of plutonium metal to thermal and mechanical perturbations is characterized by instability. Figure 1 shows plutonium's phase diagram at temperatures below its melting temperature (640°C) and at pressures below 10 kilobar. Under these relatively small changes in temperature and pressure, plutonium goes through seven distinct crystallographic phases. These solid-to-solid phase transitions arise from rearrangements of the electrons that cause the interatomic forces to weaken and the crystal structure to change.

The melting point of plutonium metal is another sign of instability, as it is very low when compared with the melting points of its neighbors in the periodic table (see Figure 2). These instabilities have been known since the forties, when Manhattan Project metallurgists struggled to fashion plutonium metal into the shape needed for the first atomic bomb, but they still baffle condensed matter physicists. Here, we report on some new measurements of atomic vibrations that shed light on both the phase instability and the melting anomaly of plutonium.

Atomic Vibrations and the Equation of State

Understanding the instabilities of plutonium and other actinides is not only of fundamental interest, but also of great practical importance for the current nuclear missions of the Department of Energy. Among those missions are cleaning up the nuclear contamination and preventing further contamination, storing nuclear waste, and maintaining a safe and reliable nuclear weapons stockpile. Foremost among the missions of Los Alamos is stockpile stewardship, which requires the construction of a reliable equation of state (EOS) for plutonium to predict the performance of nuclear weapons in the absence of weapons testing. To ensure that the EOS provides this predictive capability, we must understand the vibrational excitations of plutonium at a fundamental level because they contribute directly to the EOS.

The EOS describes the internal pressure in plutonium metal as a function of temperature and density. Plutonium metal is, of course, a solid, and its internal pressure can be divided into several contributions, whose relative sizes vary with temperature and external pressure. At $T = 0$, there is only the zero-point vibrational energy, and the pressure comes mostly from the static attraction or repulsion between the atoms. Bare nuclei repel each other, and the material flies apart. Some of the electrons surround the nuclei, forming ion cores, and screen this repulsion. Other electrons (the conduction electrons) are shared with neighboring atoms, causing the atoms to bind together. The net balance between these competing forces determines the pressure the solid can exert on its surroundings.

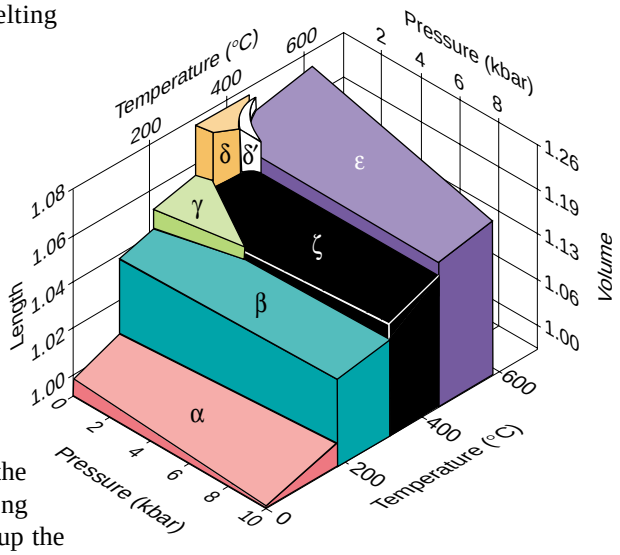

Figure 1. Pressure-Temperature Phase Diagram of Plutonium Metal
Plutonium has the most complex phase diagram of any element in the periodic table. Its seven distinct crystallographic phases arising from the rearrangements of the electrons can be stabilized with slight changes in temperature or pressure. (Reproduced with permission from the Metallurgical Society.)

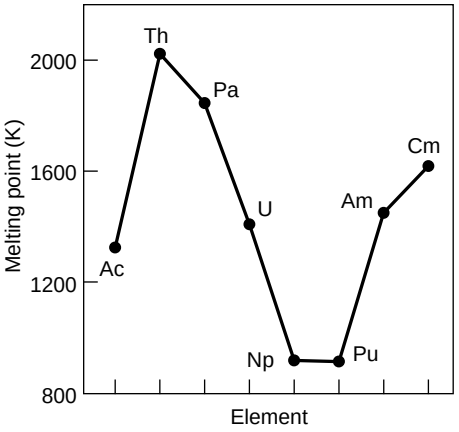

Figure 2. Melting Points of the Light Actinides
As illustrated here, the melting points of neptunium and plutonium are anomalously low by comparison with those of neighboring elements. The same is illustrated in a metallurgical context in Figure 13 in the article "Plutonium Condensed-Matter Physics" on page 61. (Reproduced with permission from *Philosophical Magazine* B80, 2000, page 53, Taylor & Francis.)

Equations of State—Theoretical Formalism

by Bard I. Bennett

Theoretical and experimental research in equations of state and material modeling is essential to ensuring a firm scientific footing for these disciplines. This type of research is necessary not only for assessing the nuclear weapons stockpile but also for developing a predictive computational capability. Here, I will outline the general theoretical formalism for calculating equations of state and then expand on the contribution from the vibrational (or thermal) excitations of solids to the equation of state (EOS). The temperature dependence of the Debye temperature reported in the main article has a direct bearing on our models for the vibrational contribution.

The EOS for any material is typically expressed as an equation for the pressure as a function of temperature and density. Generally speaking, at densities less than 100 grams per cubic centimeter (g/cm^3) and temperatures less than 100 kilo-electron-volt (keV), there are three distinct contributions to the pressure:

$$P(\rho,T) = P_c(\rho) + P_N(\rho,T) + P_e(\rho,T) \quad . \tag{1}$$

The pressure at $T = 0$, $P_c(\rho)$, is commonly called the "cold curve" and is due to the electronic forces that bind the individual atoms into a solid; $P_N(\rho,T)$ is the pressure due to the vibrational excitation of the nuclei in the solid, liquid, or gas states; and $P_e(\rho,T)$ is the pressure due to the electrons' thermal excitation.

The cold curve is traditionally modeled by empirical formulae (Lennard-Jones and Morse potentials combined with Thomas-Fermi-Dirac theory). Modern calculations of electronic band structure include relativistic effects. Experimental measurements conducted in a diamond-anvil or tungsten carbide cell can provide data for pressures up to approximately 2 megabars.

The vibrational contribution for the solid state, $P_N(\rho,T)$, is traditionally modeled with the Debye theory. Models of the liquid state use an interpolation scheme between a Debye solid and an ideal gas. Modern theory for all these states uses molecular dynamics or Monte Carlo methods to obtain pressures as a function of density and temperature. No direct experimental data are available, but to infer a melting temperature, we use shock wave methods and laser-heated diamond-anvil cells.

The pressure for electron excitations, $P_e(\rho,T)$, is traditionally modeled by Saha or Thomas-Fermi-Dirac theories. Modern theory for this contribution to the pressure uses relativistic, quantum mechanical, self-consistent field theory. No direct experimental data are available, but $P_e(\rho,T)$ can be inferred from data obtained from pressure waves generated by nuclear explosions.

We now add more detail to the vibrational contribution to pressure from the motion of the nuclei. The Mie-Grüneisen form is given by

$$P_N(\rho,T) = \rho\Gamma(\rho,T)E_N(\rho,T) \quad , \tag{2}$$

where the energy in the Debye model is given by

$$E_N(\rho,T) = \frac{3N_0k_BT}{A}\left\{D_3\left(\frac{\Theta_D}{T}\right) + \frac{3}{8}\frac{\Theta_D}{T}\right\}\left\{1 + \frac{\partial \ln \Theta_D(\rho,T)}{\partial \ln T}\right\} \quad , \tag{3}$$

and the Grüneisen parameter Γ is defined by the following equation:

$$\Gamma(\rho,T) = \frac{\int \ln \Theta_D(\rho,T)}{\int \ln \rho} \quad . \tag{4}$$

The Debye temperature $\Theta_D(\rho,T)$ is the effective atomic vibrational temperature, and it determines when a material melts or loses its strength. In Equation (3), $D_3(x)$ is the Debye integral of the third kind. In traditional EOS modeling, Θ_D is assumed to be independent of temperature—that is, $\Theta_D(\rho)$. Consequently, Γ would also be a simple function only of density. Modern theories suggest that Θ_D and Γ depend on a material's density, temperature, and electronic structure.

The neutron diffraction measurements reported in the main article confirm these theoretical ideas. The data show that the Debye temperature and the Grüneisen parameter are, indeed, a function of temperature and electronic structure.

To verify the predictions from quantum mechanical theory, we need to further validate our current models. Measuring the Debye-Waller factor with a new, heated high-pressure cell shows great promise. By using the apparatus containing this cell, we have obtained interesting data for molybdenum. After validation, the theory will be used in modeling material melting and strength for applications in weapons physics (conventional and nuclear), metal casting, or explosively driven shape-forming.

The ground-state distribution of these electrons relative to the ion cores can be predicted by electronic-structure calculations (see the article "The Ground-State Properties of the Actinide Elements: A Theoretical Overview").

As temperature increases, pressure from the vibrational motion of the ion cores increases as well. These excitations can be treated at several levels of approximation. The first two levels are the Einstein and Debye models. In both, we imagine that an external source of heat gives the ion cores an average kinetic energy, and the cores move away from their equilibrium positions, which are assumed to be fixed in space for the Einstein model and fixed to each other for the Debye model. At the same time, in both models, the electronic forces act like springs, pulling on the ions and causing them to oscillate back and forth. In the Einstein model, the ions oscillate independently of each other. Every atom vibrates at a single characteristic frequency, ω_E, and there are no propagating waves. Even though this model is unrealistically simple, it does give useful first approximations for the heat capacity and the thermal vibration amplitude. At high enough temperatures, the heat capacity is constant, and the vibration amplitude is proportional to the temperature.

Debye made the much more realistic assumption that the electronic springs attach each atom to its near neighbors in the lattice, and not to a lattice site fixed in space. Travelling waves are now allowed, and the vibrational modes (phonons), which are dictated by the crystal structure, obey different dispersion relations (frequency versus wavelength) along different crystal directions. The phonon spectrum (that is, the number of allowed vibrational frequencies per frequency interval) depends on the spacing between the crystal planes and on the atomic spring constants in those directions, but it will always be proportional to ω^2 at low frequencies. In calculating the contribution to pressure from the vibrational excitations, common practice is to use the model from Debye's theory as a starting point and extrapolate wherever necessary (see the box "Equations of State" on the opposite page).

The Debye model is a simplified description of the thermal excitations of a solid because it ignores most of the details of lattice dynamics, but it is very useful for interpreting experiments that measure the average elastic and thermal properties of a solid. (See the box "The Debye Model and the Actinides" on page 197.)

The characteristic vibrational energy of the lattice is given in temperature units by the Debye temperature. Defined as the maximum energy of any sound wave that will propagate in a periodic lattice, this energy is determined by the fact that the wavelength of sound must be greater than the lattice spacing (or lattice constant) a_0 defining the size of the crystallographic unit cell. The characteristic frequency in the Debye model is given in terms of an appropriate average sound velocity V_{sound} and the atomic volume Ω (a sphere of radius $a_0/2$):

$$\omega_D = \left(\frac{6\pi^2}{\Omega}\right)^{1/3} V_{\text{sound}} \quad . \tag{1}$$

The characteristic Debye temperature is

$$k_B\Theta_D = \hbar\omega_D \quad , \tag{2}$$

where k_B is the Boltzmann constant. The sound velocity is determined by a complicated average over the crystal direction and wave polarization:

$$V_{\text{sound}} = \Omega^{\frac{1}{3}} \left(\frac{\beta_{\text{spring}}}{m}\right)^{\frac{1}{2}} \quad , \tag{3}$$

where β_{spring} is an average atomic spring constant and m is the atomic mass. The spring constant tells how much force is required to extend the spring per unit length of extension.

The Debye theory predicts that the phonon spectrum has a simple quadratic dependence on frequency up to ω_D and then drops off discontinuously to zero. The phonon spectrum of a real crystal is more complicated but retains a quadratic behavior at low frequencies. Therefore, the Debye spectrum, characterized by Θ_D, is a reasonable improvement over the Einstein model, which has only one vibrational frequency. The point of our work is to use neutron diffraction measurements to measure Θ_D, which is essentially the same as the Debye-Waller temperature Θ_{DW}.

The Debye-Waller temperature Θ_{DW} is an average in two ways. First, it is an ω^{-2}-weighted average over all possible frequencies in the phonon spectrum, so that a measurement of the Debye-Waller temperature Θ_{DW} is equivalent to a measurement of the average elastic constant, which is equivalent to the bulk modulus B. Note that B and the average elastic constant are proportional to $\beta_{\text{spring}}/a_0$ or $\Omega^{-1/3}\beta_{\text{spring}}$. Second, Θ_{DW} is an average over all possible directions in the crystal. The Debye theory is essentially exact at low temperatures because only the low-frequency quadratic part of the phonon spectrum is excited at those temperatures. At higher temperatures, the theory is only approximate, but that approximation can be improved if Θ_D is allowed to be temperature dependent. Ultimately, we would like to measure the actual phonon spectrum rather than predict it from theory, but this is a project for the future.

At present, the question of how accurate the plutonium equation of state (EOS) is over a range of temperatures, pressures, and shock-induced conditions relevant to nuclear weapons is central to the Stockpile Stewardship Program. And our goal is to gather enough information—both experimental and theoretical—to derive the EOS from measurements of microscopic properties and first principles calculations, thereby reducing the uncertainties to a minimum. The most complete characterization of the vibrational properties could be obtained through measurements of inelastic neutron scattering on single crystals. Those measurements would determine the dispersion relations (the

dependence of vibrational frequency on wavelength) for different crystal directions. And this knowledge would provide a powerful check on the microscopic basis for the vibrational contribution to the EOS regardless of whether that contribution is calculated in the Debye or another model. Although large single crystals (about 1 cubic centimeter) needed for neutron-scattering measurements are not currently available, a significant effort is under way at Los Alamos to grow suitable crystals (see the articles "Preparing Single Crystals of Gallium-Stabilized Plutonium" and "A Single-Crystal Saga" on pages 226 and 233, respectively). In the meantime, however, ultrasonic measurements of the elastic constants will provide the directional dependence of the long-wavelength elastic constants (see the article "Elasticity, Entropy, and the Phase Stability of Plutonium on page 208).

Neutron Diffraction Studies of Atomic Vibrations

Until the large crystals required for inelastic neutron scattering become available, we are measuring polycrystalline materials. Here, we report on our neutron-powder-diffraction studies of polycrystalline samples. We measured powder diffraction patterns over a range of temperatures and fitted each measured pattern to a model of the diffraction pattern through a process known as Rietveld refinement. From the pattern of positions and intensities of the Bragg diffraction peaks at each temperature, we were able to deduce the average vibrational displacement of the nuclei from their lattice positions at that temperature and, in turn, the material's Debye-Waller temperature, Θ_{DW}. Our measurements demonstrate that Θ_{DW} varies with temperature. Indeed, by incorporating that temperature dependence into the Lindemann melting rule, we were able to predict melting temperatures for the light actinides. The theoretical and experimental values are in good agreement.

Experiments and Data Analysis

The neutron diffraction data presented in this paper were collected at the pulsed-neutron sources at Argonne National Laboratory and Los Alamos National Laboratory. We used polycrystalline samples of lead, thorium, neptunium, and plutonium encapsulated in vanadium and of uranium encapsulated in fused silica. Encapsulation is required for radiological safety. Vanadium is used for two reasons: Its coherent neutron cross-section is tiny, so its Bragg peaks are negligible, and metallurgically, vanadium is compatible with plutonium at high temperatures. The plutonium sample was highly enriched in plutonium-242 because this isotope has a very low probability of absorbing neutrons compared with the more abundant plutonium-239. Our measurements covered as much of the stability range of each phase as possible without leaving any chance for the containment to fail.

Powder diffraction is the simplest technique for obtaining crystal structures because single crystals of the material are not required. For all but the simplest structures, however, the analysis of these complex patterns can be ambiguous. Hugo Rietveld developed a method for data refinement in the late 1960s to extract precise estimates of all crystallographic parameters from x-ray and neutron-powder-diffraction patterns. In this method, the experimental data are fitted to a detailed model of the positions, intensities, and shapes of the diffraction peaks. The model accounts for the effects of the crystal symmetry, the lattice constants, the atom positions in the unit cell, and the broadening of the diffraction peaks from local crystal strain and size effects. The model also accounts for the effects of the mean-square thermal (or vibrational) displacement of the atom, $\langle u^2 \rangle$, from its equilibrium position in the crystal. The Rietveld refinement thus enables us to infer the average vibrational displacement $\langle u^2 \rangle$ from powder diffraction data. We implemented the method using the code developed by Allen Larson and Robert Von Dreele of the Los Alamos Neutron Scattering Center (LANSCE). At present, this is the most widely used computer code for Rietveld refinement in the world (Von Dreele 1990).

Figure 3 illustrates the effects of vibrational motion on the appearance of the diffraction pattern. The figure shows portions of two neutron-diffraction patterns of an aluminum-stabilized δ-phase plutonium alloy ($Pu_{0.95}Al_{0.05}$) taken at temperatures of 13 and 260 kelvins, respectively. The data are plotted as a function of *d*, the spacing between the crystallographic planes, and only the diffraction peaks at short *d*-spacings are shown. In both data sets, the Bragg diffraction peaks have the characteristic pattern produced by the face-centered-cubic structure of δ-phase plutonium. There are, however, two features that derive directly from the vibrational motion of the atoms. First, the intensities of the Bragg peaks in both data sets decrease rapidly as the *d*-spacing decreases. Second, the attenuation is noticeably stronger in the 260-kelvin diffraction pattern than in the 13-kelvin pattern.

Interpreting Diffraction Data with the Debye Theory

In 1914, Debye worked out the effect of the vibrational motion on the diffraction patterns of crystals. He showed that the intensity of a diffraction peak is proportional to an exponentially decreasing factor, now known as the Debye-Waller factor, which is given by

$$I \propto e^{-\frac{8\pi^2\langle u^2\rangle}{d^2}} . \qquad (4)$$

The negative exponent is proportional to $\langle u^2 \rangle$, implying that the intensities decrease with increasing temperature as seen in the powder diffraction data illustrated in Figure 3. Moreover, the exponent is inversely proportional to d^2, which means that the attenuation due to vibrational motion is very

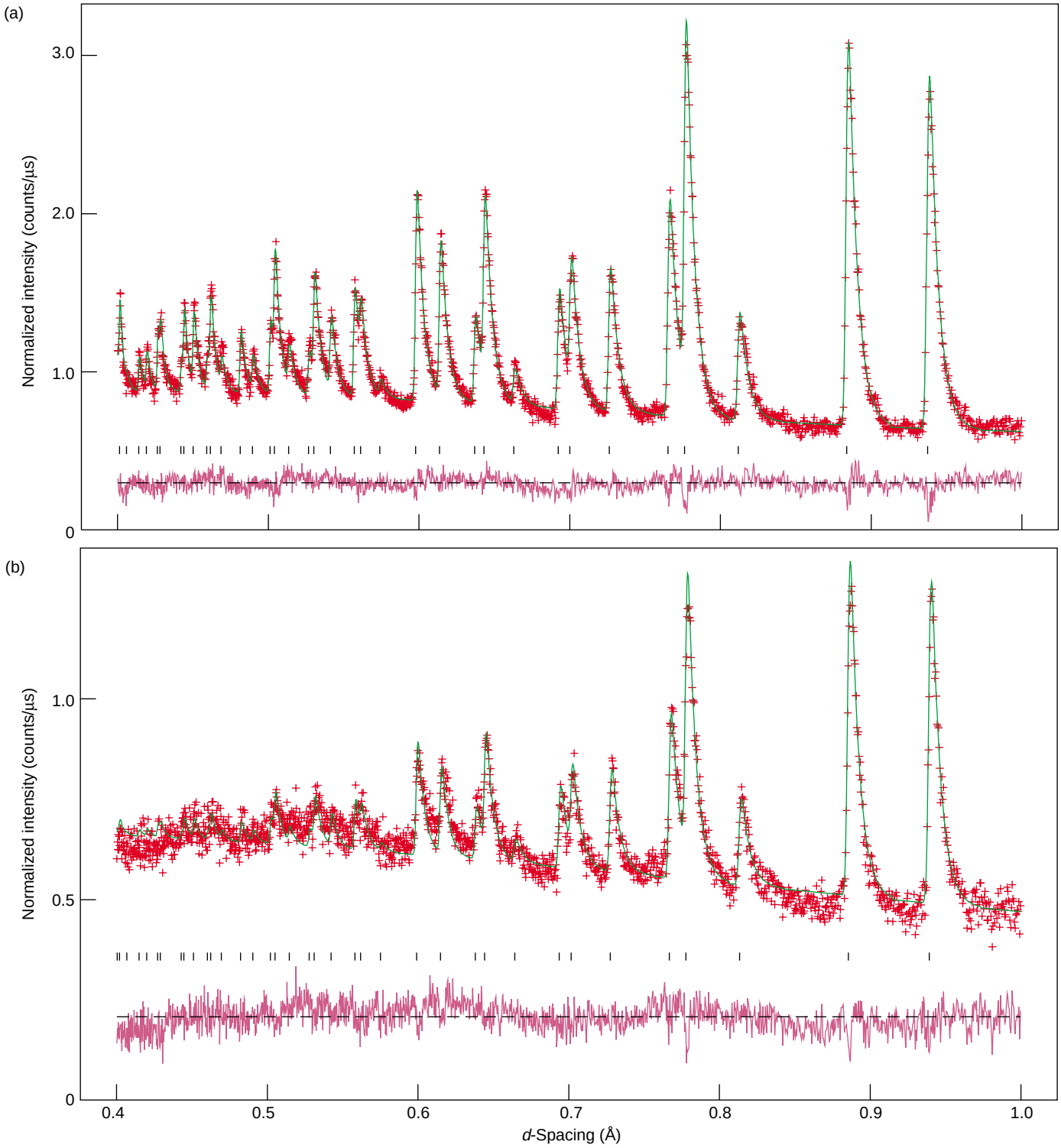

Figure 3. Neutron Diffraction Patterns for $Pu_{0.95}Al_{0.05}$

The diffraction data of the aluminum-stabilized δ-phase plutonium alloy have been fitted by Rietveld refinement. In (a), the experiment was conducted at 13 K and in (b) at 260 K. The red crosses are the observed scattered neutron intensity plotted versus crystallographic *d*-spacing, the green line through them is the Rietveld fit, and the purple curve below the data is the error of the fit. Only the short *d*-spacing portions of the patterns are shown. Notice that the Bragg peak intensities decrease from right to left as the *d*-spacing decreases. The attenuation is noticeably stronger in the 260 K than in the 13 K diffraction pattern, in keeping with the trend predicted by the Debye-Waller factor. The article describes how we deduce the Debye-Waller temperature Θ_{DW} from the Bragg peak intensities. (Reproduced with permission from *Kluwer Academic,* A. C. Lawson et al., Edited by A. Gonis et al., "Light Actinides" in *Electron Correlation and Materials Properties*, 1999, page 75.)

strongly enhanced at short *d*-spacings, also seen in Figure 3. In fact, pulsed-neutron sources such as the one at LANSCE are best suited for these powder-diffraction measurements because the neutron spectrum contains many neutrons with wavelengths at these short *d*-spacings, at which neutron diffraction scattering is most affected by the vibrational motion.

If the interatomic forces behave like harmonic springs, as they do in the Debye model, the very general equipartition law requires that each vibrational mode have $(k_B T)/2$ of energy, which means that $\langle u^2 \rangle$ increases linearly with temperature at high enough temperatures:

$$\langle u^2 \rangle = \frac{k_B T}{\beta_{\text{spring}}} \quad . \qquad (5)$$

The Debye theory for $\langle u^2 \rangle$ at low temperatures shows that the temperature dependence for $\langle u^2 \rangle$ is given by

$$\langle u^2 \rangle = \frac{3\hbar^2 T}{m k_B \Theta_{DW}^2} \times \left\{ \frac{\Theta_{DW}}{4T} + \frac{T}{\Theta_{DW}} \int_0^{\frac{\Theta_{DW}}{T}} \frac{u\,du}{e^u - 1} \right\} \quad . \qquad (6)$$

A materials constant that appears in this equation is Θ_{DW}, which as mentioned earlier, is a direct measure of the atomic spring constant β_{spring} of the material. The relationship between Θ_{DW} and β_{spring} is given by the following equation:

$$\beta_{\text{spring}} = \frac{m k_B^2 \Theta_{DW}^2}{3\hbar^2} \quad . \qquad (7)$$

Temperature-Dependent Results for Plutonium's Elastic Properties

We now describe how Θ_{DW} can be experimentally determined from measurements of $\langle u^2 \rangle$. As mentioned before, we obtain diffraction patterns over an appropriate temperature range and then apply the Rietveld refinement method to determine $\langle u^2 \rangle$ at each temperature. According to Equations (5) and (7) of the Debye model, if Θ_{DW} were a temperature-independent constant, $\langle u^2 \rangle$ should increase linearly with temperature at high temperatures, with a slope inversely proportional to Θ_{DW}^2. It should thus be easy to extract Θ_{DW} from a fit of $\langle u^2 \rangle$ versus temperature. Indeed, we have measured and analyzed many different metallic elements in this way and found that Debye's theory explains the data very well. Moreover, the measured values of Θ_{DW} are in good agreement with those determined by heat capacity measurements.

It is expected, however, that Θ_{DW} should have a slight temperature dependence, reflecting changes in the crystal's elastic properties as its volume is changed by ordinary thermal expansion. For the actinides, the thermal expansion is far from ordinary: Depending on the material, the coefficient of thermal expansion spans a wide range of values. In fact, the negative thermal expansion of unalloyed δ-phase plutonium at high temperatures is one of the unexpected properties of plutonium.

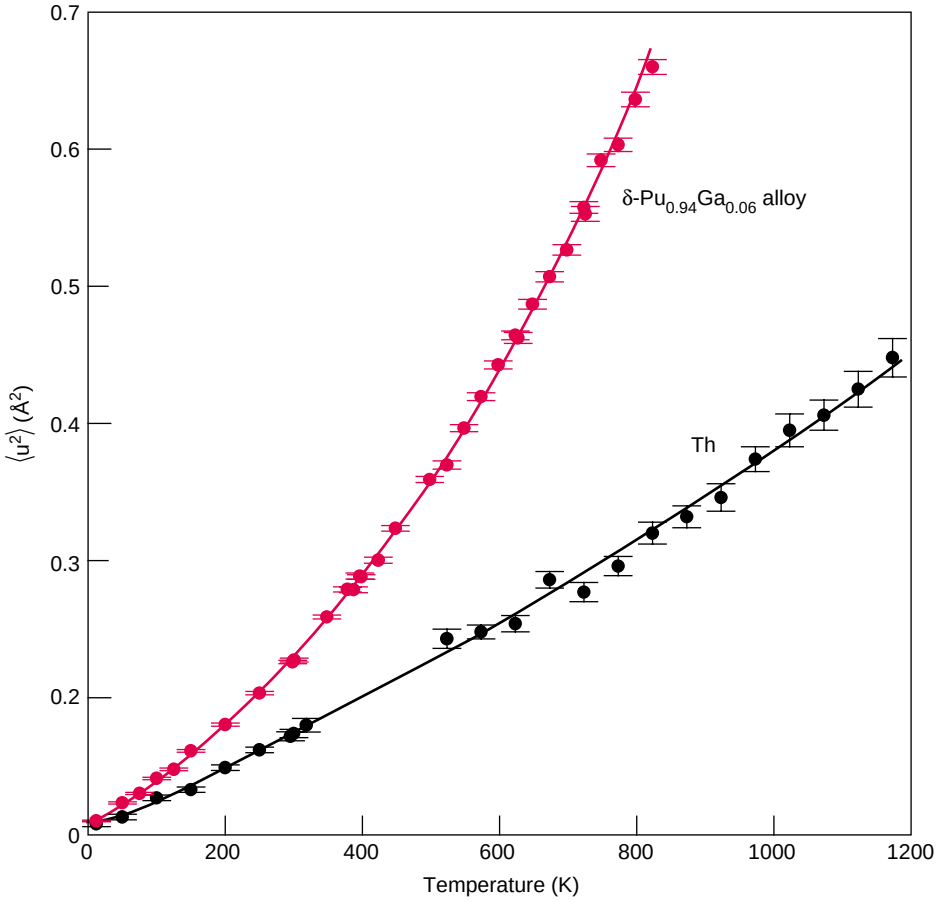

Figure 4. Mean-Square Thermal Vibration Amplitudes for δ-Phase $Pu_{0.94}Ga_{0.06}$ and Thorium Metal

Although thorium and gallium-stabilized δ-plutonium are face-centered-cubic metals, their vibrational amplitudes behave very differently as a function of temperature. As illustrated here, the linear portion of the plutonium curve is steeper than that of thorium, indicating that plutonium is more compressible (that is, its spring constant β_{spring}, which is inversely proportional to the amplitudes squared , is lower than that of thorium). At the same time, the plutonium curve displays a larger upward curvature, indicating that, at high temperature, the springs in plutonium are softening more rapidly than those in thorium.

(Reproduced with permission from *Philosophical Magazine* B80, 2000, page 53, Taylor & Francis.)

The Debye Model and the Actinides

Mechanical Assumptions of the Debye Model

- The atoms (mass m) are separated by the lattice constant (a_0) and are connected by harmonic springs, whose strengths are described by the atomic spring constant β_{spring}.
- Excitations are sound waves of wavelength λ, velocity $V_{sound} = \Omega^{1/3}(\beta_{spring}/m)^{1/2}$, where Ω *is the atomic volume*, and frequency $\omega = V_{sound}/\lambda$.
- Velocities are the same for longitudinal and transverse waves, and they are the same in all crystal directions.
- Sound waves cannot propagate if $\lambda < a_0$.
- The low-frequency sound wave (phonon) spectrum is proportional to ω^2.

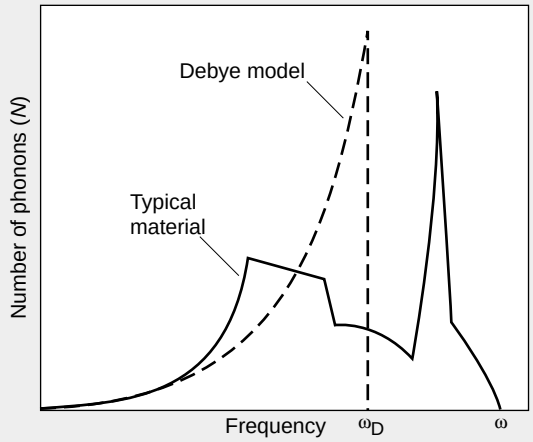

A comparison of the phonon spectra $N(\omega)$ for the Debye model (dashed line) and a typical material (solid line) shows that, whereas at low frequencies both spectra are proportional to ω^2, at high frequencies the actual spectrum of a material deviates significantly from the Debye spectrum.

Thermal Consequences of the Debye Model

If the solid has ideal, harmonic springs,

- the characteristic Debye temperature Θ_D is given by $k_B\Theta_D = \hbar(6\pi^2/\Omega)^{1/3}V_{sound}$;
- the low-temperature heat capacity is $Nk_B(T/\Theta_D)^3$, where N is the number of atoms in the solid;
- the high-temperature heat capacity is $3Nk_B$;
- the Debye temperature Θ_D is independent of temperature;
- there is no thermal expansion; and
- the solid never melts!

If the solid has weakly anharmonic springs,

- there is measurable thermal expansion;
- the spring constants depend on volume;
- the Debye temperature Θ_D depends on temperature via thermal expansion and the Grüneisen constant; and
- the melting point is approximately determined by the Lindemann criterion.

Observed Properties of the Actinides

- Thermal expansion is anomalous.
- The Debye temperature Θ_D depends strongly on temperature through an explicit temperature variation of the elastic constants.
- The melting point is anomalously low.

And yet, our measurements of Θ_{DW} held an even bigger surprise. They showed that Θ_{DW} has a very large temperature dependence. The Debye-Waller temperature decreases at a higher temperature in an approximately linear fashion. That is, Θ_{DW} obeys an equation of the approximate form

$$\Theta_{DW} = \Theta_0 + cT \quad , \qquad (8)$$

where Θ_0 is the low-temperature value of the Debye-Waller temperature and c is a small negative constant. This result means that the spring constants are effectively temperature dependent and that the springs become weaker at high temperatures. This behavior is known as elastic softening, and its effect is shown in Figure 4. In that figure, we compare our measurements of $\langle u^2 \rangle$ for δ-phase $Pu_{0.94}Ga_{0.06}$ with those for thorium metal. The two metals have the same crystal structure, but the data indicate that thorium's spring constants are stronger and much less dependent on temperature.

The curves for plutonium and thorium differ in two ways. First, the linear part of the plutonium curve is much steeper than that of thorium. The increase in slope means that plutonium is more compressible than thorium—that is, it has a lower Θ_{DW}, or atomic spring constant. Second, whereas the thorium curve is nearly linear, the plutonium curve shows a considerably upward curvature, which indicates that the atomic springs in plutonium are softening at high temperature. The experiments demonstrate directly that plutonium is more unstable than thorium, in agreement with the instabil-

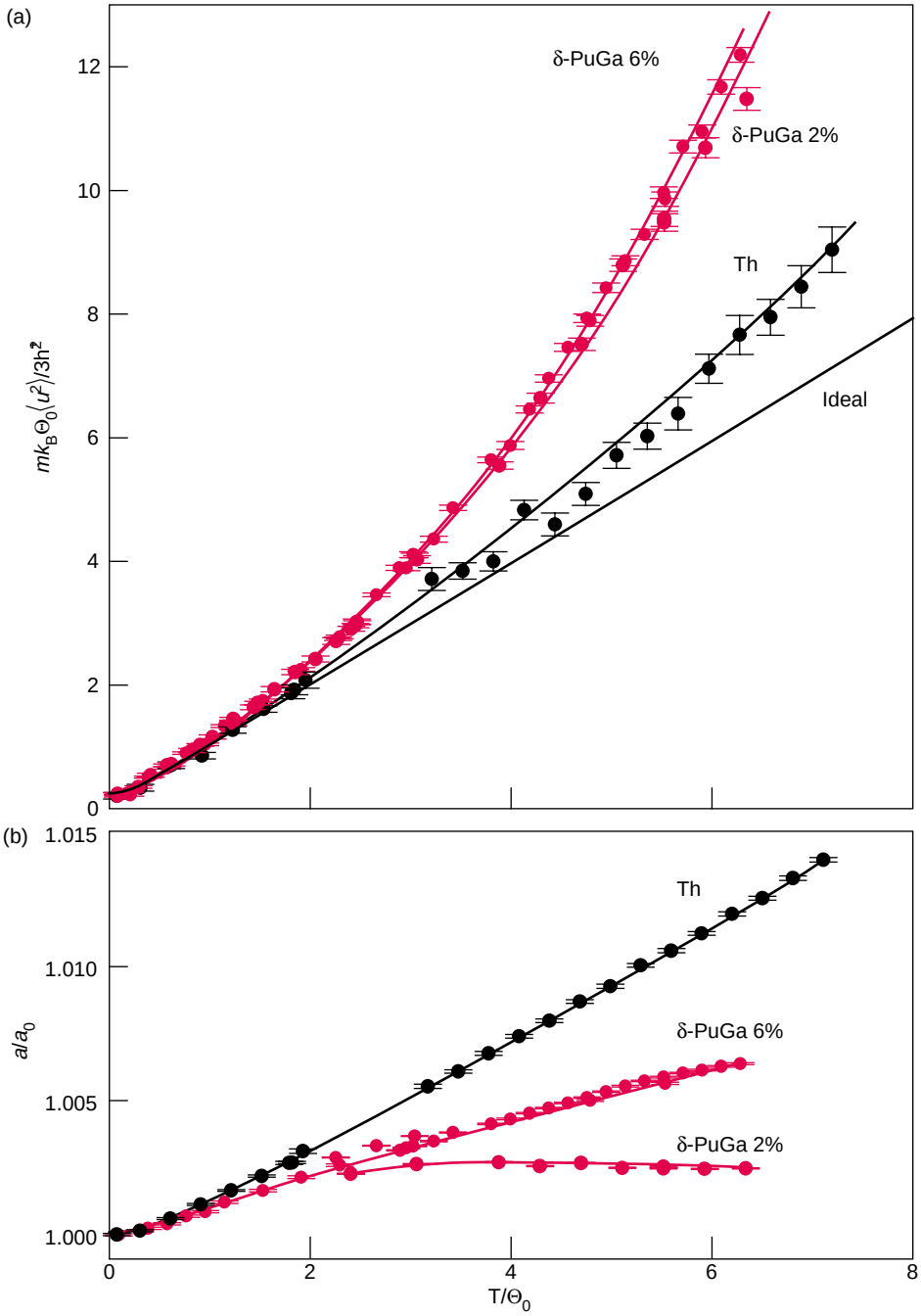

Figure 5. Dimensionless Plots of the Vibrational Displacement and Lattice Constants as a Function of Temperature

These plots are for δ-phase $Pu_{0.94}Ga_{0.06}$ and thorium metal. (a) Shown here are dimensionless displacement versus dimensionless temperature, $mk_B\Theta_0\langle u^2\rangle/3\hbar^2$ vs T/Θ_0. The ideal curve is computed from Equation (6), and it shows the universal Debye behavior for a temperature-independent Θ_{DW}, that is, $c = 0$ in Equation (8). (b) Shown here is the reduced lattice constant, a/a_0 vs T/Θ_0. The curves indicate that the thermal expansion of plutonium-gallium alloys is less than that of thorium and depends strongly on gallium concentration. The thermal expansion of the 2% sample is different from that of the 6% sample, but the corresponding vibrational-displacement course is nearly identical for these two samples. We deduce that the temperature dependence of Θ_{DW} is not a simple Grüneisen effect. (Reproduced with permission from *Philosophical Magazine* B80, 2000, page 53, Taylor & Francis.)

ities shown in Figure 1. To display these trends more clearly, we replotted the results in Figure 5 by using the dimensionless mean-square vibrational displacement, $mk_B\Theta_0\langle u^2\rangle/3\hbar^2$, versus the dimensionless temperature, T/Θ_0. Figure 5(a) shows that the temperature-induced softening of the elastic constants is quite large, and Figure 5(b) that the softening is independent of thermal expansion.

The $\langle u^2\rangle$ measurements can be used for quantifying this instability in elastic properties, and the results can be applied to modeling stockpile materials. We have observed similar softening in the other light actinides—α-uranium, α-neptunium, and α-plutonium—but not in any nonactinide material we have studied so far. From neutron diffraction measurements, we deduced the temperature dependence of Θ_{DW} for the light actinides (see Figure 6). Measurements of $\langle u^2\rangle$ are more sensitive to the behavior of the phonon spectrum at lower frequencies than are other thermal measurements, so that they reflect the portion of the phonon spectrum that is truly Debye-like. As a result, Θ_{DW} is a robust characteristic of a given material. Our findings on the temperature dependence of Θ_{DW} for δ-phase plutonium are in fair agreement with the much earlier ultrasonic measurements of Taylor et al. (1965). The observed elastic softening appears to be an intrinsic property of the light actinides.

The Melting Temperatures of the Actinides

One consequence of the measured lattice softening is that the light actinides have higher vibrational amplitudes at high temperatures than would be predicted from the low-temperature value of Θ_{DW}, that is, from a temperature-independent Θ_{DW}. That is why, we decided to reexamine the melting points of the actinides in terms of the old Lindemann melting rule.

In 1910, even before the Debye theory was proposed, Lindemann suggested that a material would melt when

the vibrational amplitude exceeds a fixed fraction f of the interatomic distance. According to Lindemann's rule, the melting point is determined by

$$T_{\text{melt}} = \frac{f^2 \Omega^{2/3} m k_B \Theta_{DW}^2}{3\hbar^2} \qquad (9)$$

where Ω is the atomic volume and f is the fractional value of the interatomic distance at which materials are supposed to melt. The melting point will appear on both sides of this equation when we substitute $\langle u^2 \rangle$ with the temperature-dependent expression for Θ_{DW} in Equation (8). For the actinides, experiment shows that f = 8.3 percent, and this value is not much different in other regions of the periodic system.

Figure 7 shows the melting points predicted from Lindemann's rule when we use the value for c deduced from experiment—see Equation (8). For melting temperatures, the agreement with experimental values is quite good. But when the temperature dependence of Θ_{DW} is ignored, the Lindemann criterion does not work at all. Thus, we should no longer consider anomalous the trend in the melting point of the actinides shown in Figure 2. Instead, we need to understand the microscopic reasons for the peculiar temperature dependence of Θ_{DW}.

We also found that, whether α-phase or stabilized δ-phase plutonium data are used in the Lindemann criterion, the predicted melting point of plutonium is almost the same. This remarkable result suggests that the melting point is an essentially atomic property.

Future Directions

Since the Debye-Waller work was completed, we have used the analysis of diffuse scattering to establish that plutonium-gallium alloys are really good Debye solids. Diffuse scattering is an oscillatory feature that appears in the background of the diffraction patterns when the motions of neighboring atoms are correlated, and these features are

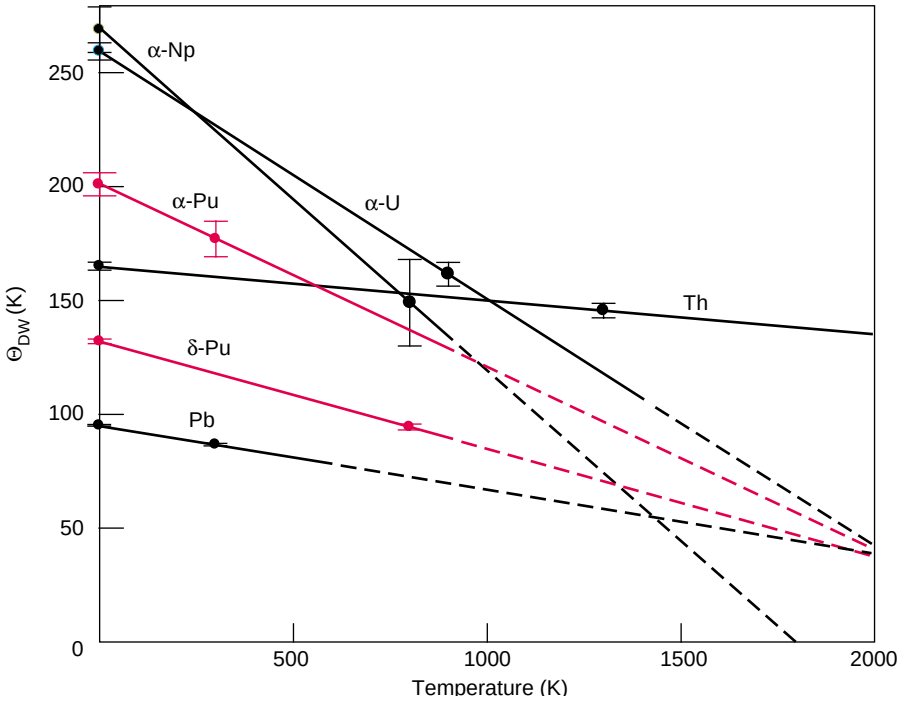

Figure 6. Temperature Dependencies of Θ_{DW} for the Light Actinides

Results from our neutron-diffraction measurements show the temperature dependence of Θ_{DW} for the light actinides. The lines span the temperature range of the solid phases. The intercept of each line shows Θ_{DW} at T = 0, and the slope shows the elastic softening observed for each material. This elastic softening is an intrinsic property of the light actinides. (Reproduced with permission from *Kluwer Academic*, A. C. Lawson et al., Edited by A. Gonis et al., "Light Actinides" in *Electron Correlation and Materials Properties*, 1999, page 75.)

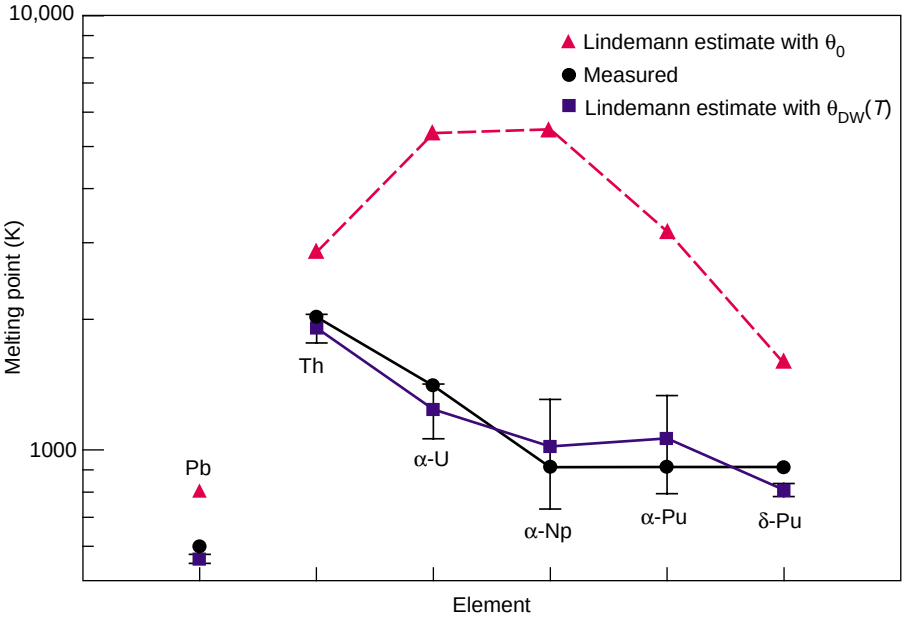

Figure 7. Melting Points of the Light Actinides

The melting points of the light actinides were determined in three ways: from experiment (black dots), from the Lindemann estimate of the melting point based on Θ_0, the low-temperature value of Θ_{DW} (red triangles), and from the Lindemann estimate based on the temperature-dependent Θ_{DW} (blue rectangles). Experimental data and the estimate based on the temperature-dependent Θ_{DW} are in good agreement.

actually visible in the data of Figure 3 (see error curve). The analysis shows that diffuse scattering is in good agreement with the Debye model and that the measured correlations are exactly as expected when the atoms are coupled to each other (the Debye model) rather than to fixed lattice sites (the Einstein model).

The next stage of this work is the difficult task of extending the measurements to high pressure. In effect, we will be using neutrons to make high-pressure elasticity measurements. Also in future years, single crystals will become available, and very detailed phonon-dispersion measurements will be completed. Those measurements will supersede the ones we have reported here by mapping out the dependence of vibrational energy on wavelength and crystal direction. They will enable us to relate important properties of stockpile materials, such as melting, to their fundamental origins in the properties of the 5f electrons present in the actinides. ■

Further Reading

Debye, P. 1914. *Annalen der Physik* **43**: 49. Reprinted in Peter J. W. Debye. 1988. *The Collected Works*. Woodbridge, CT: Oxbow Press. 3.

Lawson, A. C., J. A. Goldstone, B. Cort, R. Sheldon, and E. Foltyn. 1994. Debye-Waller Factors of the Light Actinide Elements. In *Actinide Processing: Methods and Materials.Proceedings of an International Symposium Held at the 123rd Annual Meeting of the Minerals, Metal, and Materials Society.* Edited by B. Mishra and W. A. Averill. Warrendale, PA: TMS. 31.

Lawson, A. C., B. Martinez, J. A. Roberts, B. I. Bennett, and J. W. Richardson, Jr. 2000. *Phil. Mag*. **B80**: 53.

Lindemann, F. A. 1910. *Phys. Z.* **11**: 609.

Stephens, P. W. 1999. *J. Appl. Crystallogr*. **32:** 281.

Taylor, J. C., R. G. Loasby, J. D. Dean, and P. F. Linford. 1967. Some Physical Properties of Plutonium at Low Temperatures. In *Plutonium 1965. Proceedings of the Third International Conference on Plutonium*. Edited by A. E. Kay M. B. Waldron. London: Chapman and Hall Ltd.

Von Dreele, R. B. 1990. *Los Alamos Science* **19**: 132.

Bard I. Bennett received his Ph.D. in theoretical solid-state physics from the University of California at Irvine. Currently, he is the Program Manager for Nuclear Emergency and Proliferation. Bard has over 23 years of experience in equation of state and opacity theories with particular emphasis on the application of these theories to the design of nuclear weapons. As codeveloper of the SESAME equation of state and Opacity Data Library, he has been involved in the design of many Los Alamos nuclear tests.

Andrew C. Lawson received his undergraduate degree in physics from Pomona College and his Ph.D. from the University of California (U.C.) at San Diego, where he was in Bernd Matthias's superconductivity group. After a postdoctoral stint at UC San Diego, Lawson taught physics at Pomona College and mechanical engineering at California State University at Long Beach. Lawson then joined the Physical Metallurgy Group at Los Alamos and now works in the Structure and Properties Group of the Materials Science and Technology Division. His research interests cover the study of actinide materials with neutron and x-ray diffraction.

Barbara Martinez received her B. S. and M. S. degrees in physics from Stephen F. Austin State University. She received her Ph. D. in physics from Texas A&M University, where she studied phase transitions in low-dimensional organic metals at low temperatures. She joined the Los Alamos National Laboratory as a Director-funded postdoctoral fellow in 1980 and is now a technical staff member in the Chemistry, Metallurgy, and Materials Group. Her research interests include transport and magnetic properties, phase transitions, and aging effects in plutonium and other actinide materials.

James W. Richardson, Jr. received his B.S. degree from Purdue University and his Ph.D degree from Iowa State University. Richardson is a materials scientist in the Intense Pulsed Neutron Source Division at Argonne National Laboratory and has over 15 years of experience in neutron and x-ray diffraction. He is recognized for his work in structure solutions of microporous zeolites and molecular sieves from neutron powder diffraction. Richardson developed novel analysis techniques for mixed crystalline/amorphous systems and has conducted in situ diffraction studies of industrial materials and processes, as well as nonambient (neutron irradiation) structural studies of transuranic intermetallics. He has more than 70 publications and is a corecipient of a 1992 Federal Laboratory Consortium Special Award for Excellence in Technology Transfer for determining strain by neutron diffraction.

Joyce A. Roberts received her undergraduate degree in physics from Syracuse University and her Ph.D. on radiation damage in materials at the State University of New York at Stony Brook. She joined Los Alamos as a postdoctoral fellow in 1981. In 1990, she was appointed Deputy Leader of the Manuel Lujan Jr. Neutron Scattering Center. She has been responsible for the construction of the Neutron Powder Diffractometer at the Manuel Lujan Jr. Neutron Scattering Center. Roberts's research interests include the structure of actinide materials, actinide and other metal hydrides, superconductors, binary alloys, and strain in composite materials measured by neutron and x-ray diffraction techniques.

Microstrain in δ′-Plutonium

Andrew C. Lawson

In addition to giving information on crystal structure, the shapes of the diffraction peaks also give valuable information on other aspects of the state of the material. In particular, if the lattice "constant" is not really constant but actually fluctuates throughout the bulk material, then the diffraction lines will be broadened. One mechanism for fluctuation is the strain caused by the forces exerted by the grains on one another in the course of a crystallographic transformation.

Thanks to the analysis developed recently by Peter Stephens, it is now possible to include anisotropic microstrain broadening in the Rietveld analysis. This means that one allows for the strain in individual grains to depend on crystal direction. The observed microstrain, which is an average over many grains, is a distribution that must be consistent with the crystal symmetry. The observed microstrain in δ′-plutonium is shown in Figure 1. The figure indicates that the spread in the distribution of lattice spacings is much greater in the crystallographic *c*-direction of the tetragonal crystals of δ′-plutonium than in the *a*-direction.

Why is the microstrain so high for δ′-plutonium? We do not know in detail, but it would seem that the tetragonal δ'-structure is a rather unhappy compromise between the two cubic structures, δ and ε (Figure 2).

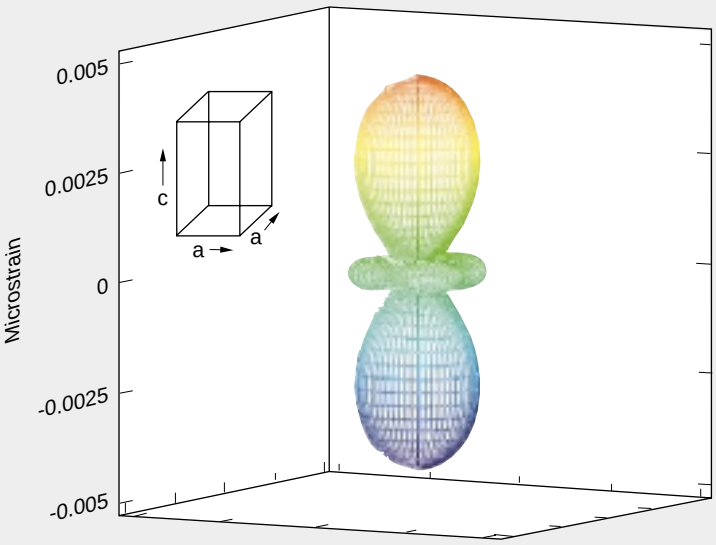

Figure 1. Anisotropic Microstrain for δ′-Plutonium at 740 K

This plot shows the root-mean-square average deviation of the crystal *d*-spacings in δ′-Pu plotted versus crystal direction. This quantity is called the microstrain, and it is determined by intergranular stresses. In the tetragonal crystal shown here, the microstrain is much larger in the crystallographic *c*-direction. The microstrains are caused by intergranular stresses.

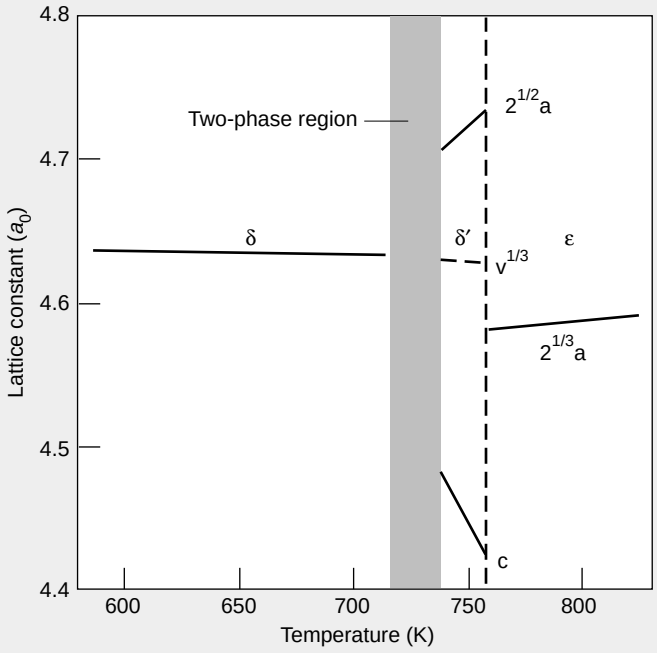

Figure 2. Temperature Dependence of the Normalized Lattice Constants of Pure Plutonium

Between 600 and 800 K, plutonium transforms from face-centered-cubic δ′-phase to face-centered-tetragonal δ′-phase and then to body-centered-cubic ε-phase. Even though they are both cubic, the structures of the δ′- and ε-phases are not closely related to each other, and the atomic volumes are very different. The interatomic distances have to change considerably during the transformation, and this change leads to a large microstrain for the tetragonal δ′-phase. **(Reproduced with permission from *Kluwer Academic*, A. C. Lawson et al., Edited by A. Gonis et al., "Light Actinides" in *Electron Correlation and Materials Properties*, 1999, page 75.)**